Title

n' PRODUCTION IN n+d INTERACTIONS FROM THRESHOLD TO 2.4 GeV/c

Authors

Rader, Robert K.
Abolins, Moris A.
Dahl, Orin I.
et al.

Publication Date

1972-07-01

Published by Physical Review D
6 pp. 3059-3068, 1972

LBL-1550
c.1

η' PRODUCTION IN $\pi^+ d$ INTERACTIONS FROM THRESHOLD TO 2.4 GeV/c

Robert K. Rader, Maris A. Abolins,
Orin I. Dahl, Jerome S. Danburg, Donald W. Davies
Paul L. Hoch, Janos Kirz, and Donald H. Miller

July 1972

Prepared for the U.S. Atomic Energy Commission
under Contract W-7405-ENG-48

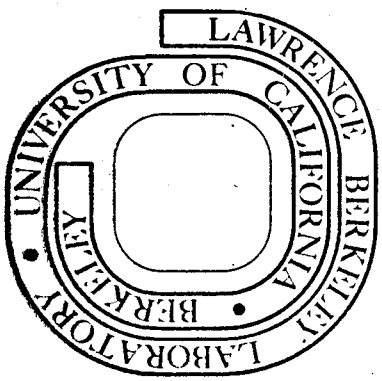

LBL-1550
c.1

DISCLAIMER

Reprinted from:

PHYSICAL REVIEW D VOLUME 6, NUMBER 11 1 DECEMBER 1972

η' Production in $\pi^+ d$ Interactions from Threshold to 2.4 GeV/c*

Robert K. Rader,† Maris A. Abolins,‡ Orin I. Dahl, Jerome S. Danburg,§ Donald W. Davies,‖ Paul L. Hoch, Janos Kirz,** and Donald H. Miller††

Lawrence Berkeley Laboratory, University of California, Berkeley, California 94720

(Received 11 July 1972)

We have studied η' production using a π^+ beam incident on deuterium in the 72-in. bubble chamber, with beam momenta from 1.1 to 2.4 GeV/c. Cross sections for reactions leading to five- and six-pronged final states are presented. We observe η' production in the reaction $\pi^+ d \to pp\eta'$, with the decay mode $\eta' \to \pi^+\pi^-\eta$. The cross section for $\pi^+ n \to p\eta'$ (studied in the impulse approximation) is observed to rise to a maximum of about 100 μb at 2.2-GeV c.m. energy. The production angular distribution develops peripheral peaking with increasing energy.

I. INTRODUCTION

We have studied η' production in $\pi^+ d$ interactions as part of a 250 000-picture bubble-chamber experiment, performed in the deuterium-filled 72-in. bubble chamber, at the Lawrence Berkeley Laboratory. We used a π^+ beam from the Bevatron at beam momenta from 1.1 to 2.4 GeV/c, in approximately 0.2 GeV/c steps. The experiment was designed to study the production of the $I=0$, nonstrange mesons in $\pi^+ n$ interactions from 1.7- to 2.4-GeV center-of-mass (c.m.) energy.

The reactions $\pi^- p \to nX$ (where $X = \eta$, ω, or η') are difficult to analyze in hydrogen-bubble-chamber experiments, as there are two neutral particles in the final state (with unmeasured momenta) and the kinematic fits to the reactions are unconstrained. However, the charge-symmetric reactions $\pi^+ n \to pX$ can be studied in deuterium.

The observed η and ω production is reported in Ref. 1. Strange-particle and ϕ-meson production have been studied and are reported in Ref. 2. For further references to work published from this experiment, and other $\pi^+ d$ studies, see the compilation in Ref. 1.

In this paper we study the reaction $\pi^+ d \to p_s p\eta'$, $\eta' \to \pi^+\pi^-\eta$. The subsequent η decay $\eta \to \pi^+\pi^-\pi^0$ or $\pi^+\pi^-\gamma$ yields five- or six-pronged events (depending on the range of the spectator proton, p_s, in the deuterium) while the decay mode $\eta \to$ neutrals is observed among three- or four-pronged events.

Special interest in η' production in pion-nucleon interactions was generated in early 1966, when it was pointed out that the decay $\eta' \to \pi^+\pi^-\gamma$ is a good place to look for a violation of charge-conjugation invariance in electromagnetic decays.[3] To plan an experiment using the reaction $\pi^- p \to n\eta'$, it is helpful to know the cross section for this process. One of the goals of the present experiment was the determination of the η' cross section and production angular distribution as a function of beam energy.

The experimental details are discussed in Sec. II. Cross sections for the five- and six-pronged final states are presented in Sec. III. (The corresponding data from the three- and four-pronged events are presented in Ref. 1.) Results on η' production are given in Sec. IV.

II. EXPERIMENTAL PROCEDURES

A. Beam Momenta and Pathlengths

The experiment[4] was run at eight beam-momentum settings, from 1.1 to 2.4 GeV/c in steps of about 0.2 GeV/c. Because of the Fermi motion of the nucleons in the deuteron, this completely covers the c.m. energy range for the reactions on a nucleon from 1.7 to 2.4 GeV. The median values of the beam momenta at the center of the chamber were determined experimentally from four-pronged events fitted with four constraints. (About 700 events were used at each momentum.) The beam momenta and pathlengths are given in Table I. Our estimated proton contamination is $\lesssim 5\%$; our estimated noninteracting (μ^+) beam contamination is $\lesssim 10\%$.

B. Scanning and Measuring

The film was scanned for nonstrange events (three-, four-, five-, and six-pronged events). The five- and six-pronged events were measured on a Franckenstein measuring projector, and the three- and four-pronged events were measured on a Spiral Reader.[5]

TABLE I. Beam momenta and pathlengths.

Beam momentum (GeV/c)	Total pathlength [a] (events/μb)
1.10	0.45 ± 0.03
1.30	0.44 ± 0.03
1.53	2.53 ± 0.13
1.58	0.43 ± 0.04
1.70	3.03 ± 0.16
1.86	2.92 ± 0.15
2.15	3.09 ± 0.13
2.37	0.84 ± 0.08

[a] The effective pathlength for accepted events is about 20% lower due to scanning and reconstruction inefficiency.

C. Geometric Reconstruction and Kinematic Fitting

We used the program TVGP[6] for geometric reconstruction of particle tracks, and SQUAW[7] for kinematic fitting to final-state hypotheses.

Unseen (spectator) protons were assigned a measured momentum of $(P_x, P_y, P_z) = [(0,0,0) \pm (30,30,40)]$ MeV/c. If there are no missing particles, the resulting pseudo-four-constraint fit reproduces the expected spectator momentum distribution reasonably well. If there is one missing particle, the resulting pseudo-one-constraint fit systematically underestimates the spectator momentum: At best, the fit can only determine the projection of the spectator momentum on the measured value for the total missing momentum.

Events which failed geometric or kinematic reconstruction were remeasured; the five- and six-pronged events which failed again were examined on the scan table. Events which had been incorrectly classified as five- or six-pronged events (e.g., a four-pronged event with a Dalitz pair) were reassigned to their correct topology; events which were not measurable (too many scatters, too many short tracks, vertex obscured) were tagged as unmeasurable. The cycle of remeasurement and failure checking was repeated for the five- and six-pronged events until they were either successfully reconstructed or identified as unmeasurable.

III. CROSS SECTIONS FROM FIVE- AND SIX-PRONGED EVENTS

A. Final States and Deuteron Cross Sections

The five- and six-pronged events[8] were fitted to the following reaction hypotheses:

$$\pi^+ d \to pp\pi^+\pi^+\pi^-\pi^- \quad (1)$$

$$\to pp\pi^+\pi^+\pi^-\pi^-\pi^0 \quad (2)$$

$$\to pp\pi^+\pi^+\pi^-\pi^-\gamma \quad (3)$$

$$\to pp\pi^+\pi^+\pi^-\pi^- \quad (\mathrm{MM} \geq \pi^0\pi^0) \quad (4)$$

$$\to pn\pi^+\pi^+\pi^+\pi^-\pi^- \quad (5)$$

$$\to p\pi^+\pi^+\pi^+\pi^-\pi^- \quad (\mathrm{MM} \geq n\pi^0) \quad (6)$$

$$\to d\pi^+\pi^+\pi^+\pi^-\pi^- \quad (7)$$

$$\to \pi^+\pi^+\pi^+\pi^+\pi^-\pi^- \quad (\mathrm{MM} \geq nn), \quad (8)$$

where MM stands for missing mass. [Reactions (7) and (8) were tried only for six-pronged events. Only two events of each type were found; they are not considered further.]

The separation of these hypotheses is discussed at length in Ref. 4. The following conclusions were reached:

(a) We cannot completely separate hypotheses (2) and (3); in cases of ambiguity fits to reaction (2) have been used, since reaction (3) occurs much less often.

(b) We estimate that contamination of hypotheses (2) and (3) by other reactions is <5%, and that loss from these final states into all other final states is <5%.

(c) We estimate that contamination of hypotheses (2) and (3) by fits with a π^+ and proton track interchanged is $\lesssim$2%, as this is the fraction of self-ambiguous events for this final state.

The number of events assigned to final states (1)–(6) and the corresponding cross sections are presented in Table II as a function of beam momentum. The cross section values shown have been corrected for scanning efficiency, reconstruction efficiency, and the effect of cuts on fiducial volume.

B. Nucleon Cross Sections

1. *The Spectator Model*

The spectator model of the interaction of the incident pion with the deuteron can be described simply in this way: The pion interacts with only one nucleon, and the other proceeds with its original momentum, merely a spectator to the interaction. We take as the "spectator" nucleon the one with the lower momentum in the laboratory.

There are two phenomena which affect cross section determinations in deuterium. These are the Glauber (screening) correction, and the suppression of certain momentum states by the Pauli Exclusion Principle. These effects are too small to be of importance in view of the level of statistics in this study; see, however, the discussion in Ref. 1.

TABLE II. Cross sections (μb) for five- and six-pronged final states in $\pi^+ d$ reactions.

Reaction	Beam momentum (GeV/c) 1.10 σ	Events	1.30 σ	Events	1.53 σ	Events	1.58 σ	Events	1.70 σ	Events	1.86 σ	Events	2.15 σ	Events	2.37 σ	Events
$\pi^+ d \to pp\pi^+\pi^+\pi^-\pi^-$	7±5	2	26±8	10	60±7	113	101±2	33	132±12	311	194±17	438	339±27	768	443±55	266
$\pi^+ d \to pp\pi^+\pi^+\pi^-\pi^-\pi^0/\gamma$					9±2	16	12±6	4	26±4	61	59±7	134	152±13	345	253±34	152
$\pi^+ d \to pp\pi^+\pi^+\pi^-\pi^-$MM ($MM \geq \pi^0\pi^0$)					1±1	1			1±1	3	4±1	10	9±2	20	8±4	5
$\pi^+ d \to pn\pi^+\pi^+\pi^+\pi^-\pi^-$					2±1	3			6±2	14	11±2	26	45±5	103	70±13	42
$\pi^+ d \to p\pi^+\pi^+\pi^+\pi^-\pi^-$MM ($MM \geq n\pi^0$)									1±1	2	2±1	5	9±2	21	18±6	11

2. *Comparison of Data with Spectator Model*

The distribution of the 3-momentum of the nucleons in the deuteron is taken to be the Hulthén wave-function prediction

$$p^2\phi^2(p) \propto p^2\left(\frac{1}{p^2+\alpha^2}-\frac{1}{p^2+\beta^2}\right)^2 . \tag{9}$$

The value of α is determined by the deuteron binding energy to be $\alpha = 0.0457$ GeV/c. In the literature β has been taken to be 7α (Ref. 9) and 5.18α (Ref. 10). We have used $\beta = 5.18\alpha$; none of our results is sensitive to the value of β.

Figure 1 shows the spectator momentum distribution for all events from reaction (1), which is a four-constraint fit. The curve is the spectator model prediction (Hulthén distribution), normalized to fit the data below 250 MeV/c. The fraction of events with spectator momentum over 250 MeV/c is 34%. The nucleons in the deuteron have a Fermi momentum greater than 250 MeV/c only 2–7% of the time (the number is not well known),[11] so it is clear that the majority of high-momentum spectators are not spectators to the scattering at all – both nucleons have been struck. Such events are not described by the spectator model. We thus require that the spectator momentum be less than 250 MeV/c when using this model to obtain πN cross sections. There is quite reasonable agreement between the data and the curve below 250 MeV/c. *For the remainder of this paper we will consider only events satisfying this condition;* we will correct the πN cross sections obtained to account for the excluded events. We note that we found no evidence that the excluded high-spectator momentum events are more likely to be misidentified events than the rest.

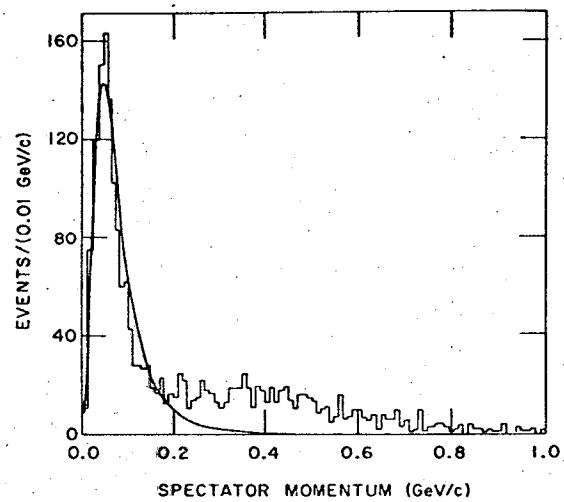

FIG. 1. Comparison of spectator model with data from the reaction $\pi^+ d \to pp\pi^+\pi^+\pi^-\pi^-$ (1936 events).

TABLE III. Center-of-mass energy bins and pathlengths.

Central value (GeV)	Bin limits (GeV)	Total pathlength [a] (events/μb)
(Underflow)	1.68	0.06
1.73	1.68–1.78	0.45 ± 0.03
1.84	1.78–1.88	0.63 ± 0.04
1.94	1.88–1.98	2.77 ± 0.15
2.02	1.98–2.06	3.06 ± 0.17
2.11	2.06–2.16	3.01 ± 0.15
2.22	2.16–2.28	2.86 ± 0.13
2.33	2.28–2.42	0.90 ± 0.07
(Overflow)	2.42	0.02

[a] The effective pathlengths for accepted events satisfying the spectator cut $P_s < 250$ MeV/c are about 40% smaller.

3. *Calculation of the Nucleon Cross Sections vs c.m. Energy*

The pathlengths at each of the several beam momenta are known (Table I) and the spectator model is used to calculate the distribution of pathlength in c.m. energy. The c.m. energy of the beam and the struck nucleon is given by

$$E_{\text{c.m.}} = [(p_b + p_d - p_s)^2]^{1/2}. \tag{10}$$

Here p_b, p_d, p_s are 4-momenta, and the subscripts b, d, and s refer to the beam, deuteron, and spectator, respectively. The nucleons in the deuteron are assumed to be moving in a random direction with equal and opposite 3-momenta distributed according to the Hulthén distribution given above. The probability of a collision is weighted by the invariant flux factor of Møller,[12]

$$\text{Flux}(p_b, p_t) = [(p_b \cdot p_t)^2 - m_b^2 m_t^2]^{1/2}/m_b m_t, \tag{11}$$

where $p_t = p_d - p_s$ is the 4-momentum of the target.

The pathlength values at the incident momenta given in Table I were distributed in c.m. energy according to the Hulthén momentum distribution and the Møller flux factor using numerical integration. The calculated pathlength in several c.m. energy intervals is given in Table III.

The number of events assigned to each $\pi^+ N$ reaction has been tallied by c.m. energy; these numbers are given in Table IV. To determine the correction for high-spectator-momentum events we distribute all events in c.m. energy bins in the same way that the pathlength was distributed; the same process is applied to the high-spectator-momentum events. The fraction of high-spectator-momentum events can then be calculated for each reaction and c.m. energy bin. This procedure

TABLE IV. Cross sections (μb) for $\pi^+ n$ reactions.

Reaction	Center-of-mass energy (GeV) 1.73 σ	1.73 Events	1.84 σ	1.84 Events	1.94 σ	1.94 Events	2.02 σ	2.02 Events	2.11 σ	2.11 Events	2.22 σ	2.22 Events	2.33 σ	2.33 Events
$\pi^+ n \to p\pi^+\pi^+\pi^-\pi^-$	12 ± 9	2	30 ± 10	9	55 ± 8	70	123 ± 13	179	204 ± 19	305	343 ± 29	485	485 ± 57	234
$\pi^+ n \to p\pi^+\pi^+\pi^-\pi^-\pi^0/\gamma$					8 ± 3	11	27 ± 5	39	56 ± 8	81	145 ± 15	188	294 ± 39	125
$\pi^+ n \to p\pi^+\pi^+\pi^-\pi^-$ MM ($\text{MM} \geq \pi^0\pi^0$)							2 ± 1	3	4 ± 2	3	6 ± 2	6	16 ± 7	6
$\pi^+ n \to n\pi^+\pi^+\pi^+\pi^-\pi^-$, or $\pi^+ p \to p\pi^+\pi^+\pi^+\pi^-\pi^-$					1 ± 1	1	4 ± 2	3	13 ± 4	13	40 ± 7	41	97 ± 20	29

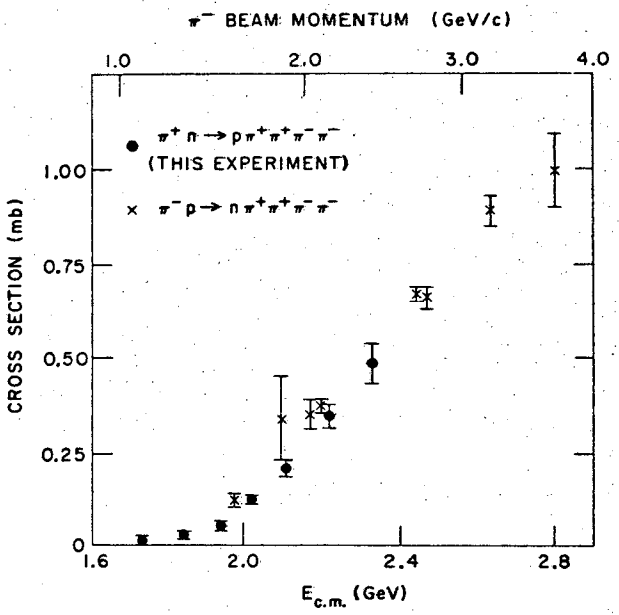

FIG. 2. Cross section for $\pi^+n \rightarrow p\pi^+\pi^+\pi^-\pi^-$ from this experiment, and for the charge-symmetric reaction $\pi^-p \rightarrow n\pi^+\pi^+\pi^-\pi^-$ from other sources (Ref. 13).

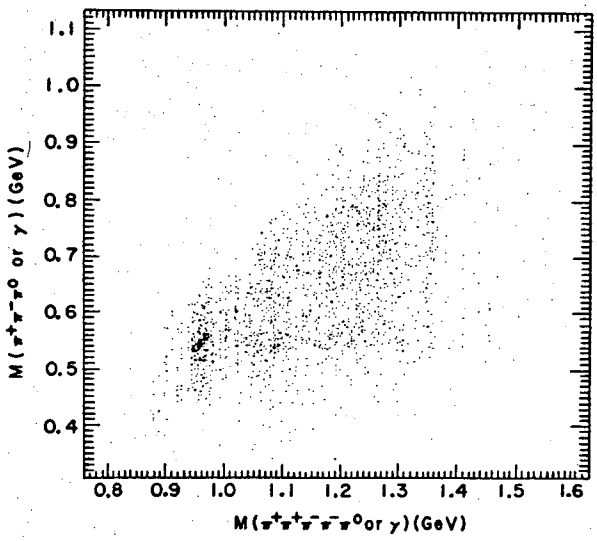

FIG. 3. $M(\pi^+\pi^-$ neutral) vs $M(\pi^+\pi^+\pi^-\pi^-$ neutral) where the neutral is a π^0 or γ (4 combinations for each of 451 events).

yields the probability of a rescattering of one of the final-state particles with the spectator nucleon, assuming that the high-spectator-momentum events are due to such a rescattering.

The cross sections, corrected for the cut on high-spectator-momentum events, have been calculated and are shown in Table IV. Reaction (5) has a neutron spectator 59% of the time, averaged over all c.m. energies; the cross section given is the sum of the $\pi^+n \rightarrow n\pi^+\pi^+\pi^+\pi^-\pi^-$ and $\pi^+p \rightarrow p\pi^+\pi^+\pi^+\pi^-\pi^-$ cross sections.

Our determination of the $\pi^+n \rightarrow p\pi^+\pi^+\pi^-\pi^-$ cross section is shown in Fig. 2. Charge-symmetric data for the reaction $\pi^-p \rightarrow n\pi^+\pi^+\pi^-\pi^-$ are also shown; these data are compiled from many experiments.[13] The agreement between the two sets of data justifies the above procedure for cross-section determination.

IV. η' PRODUCTION

A. Known Properties of the η' Meson

The η' meson was discovered in K^-p experiments in 1964.[14,15] Its mass is 957.5 ± 0.8 MeV, and its quantum numbers are $I^G = 0^+$ and $J^P = 0^-$ (or 2^-).[16,17] The η' decays into the state $\pi\pi\eta$ 64% of the time.[17] Using the known neutral-to-charged branching ratio of the η meson, and the fact that the $(\pi\pi)_{I=0}$ state is $\pi^+\pi^-$ two-thirds of the time, the branching ratios of the η' into the various final states are calculated to be

$$\eta' \rightarrow \pi^+\pi^- (\eta \rightarrow \text{neutrals}) \quad (32\%) \quad (12)$$

$$\rightarrow \pi^+\pi^- (\eta \rightarrow \pi^+\pi^-\pi^0 \text{ or } \pi^+\pi^-\gamma) \quad (13\%) \quad (13)$$

$$\rightarrow \pi^0\pi^0 (\eta \rightarrow \pi^+\pi^-\pi^0 \text{ or } \pi^+\pi^-\gamma) \quad (6\%) \quad (14)$$

$$\rightarrow \pi^+\pi^-\gamma \quad (29\%) \quad (15)$$

$$\rightarrow (\text{neutrals}) \quad (20\%). \quad (16)$$

The η' has also been observed in the reactions $\pi^+p \rightarrow \Delta^{++}\eta'$,[18] $\pi^-p \rightarrow n\eta'$,[19-21] and $\pi^+d \rightarrow pp\eta'$.[22-24] The amplitudes for the reactions $\pi^-p \rightarrow n\eta'$ and $\pi^+n \rightarrow p\eta'$ should be equal, by the charge symmetry of strong interactions.

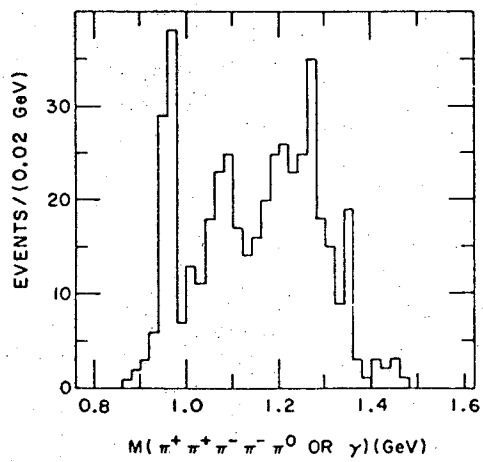

FIG. 4. Mass of $\pi^+\pi^+\pi^-\pi^-\pi^0/\gamma$, from the reactions $\pi^+d \rightarrow pp\pi^+\pi^+\pi^-\pi^-\pi^0/\gamma$ (451 events).

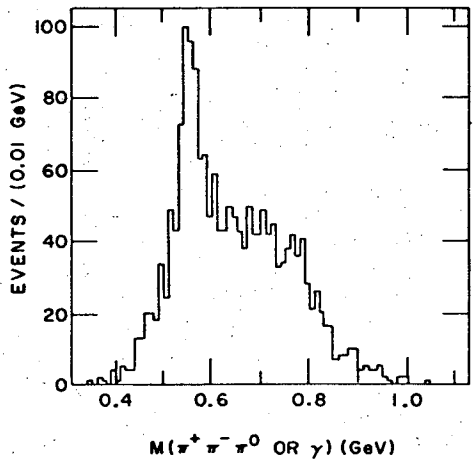

FIG. 5. Mass of $\pi^+\pi^-\pi^0/\gamma$, from reactions $\pi^+d \to pp\pi^+\pi^+\pi^-\pi^-\pi^0/\gamma$ (four combinations for each of 451 events).

B. η' Production in Five- and Six-Pronged Events

The final state $pp\pi^+\pi^+\pi^-\pi^-(\pi^0/\gamma)$ has been studied for evidence of η' production in π^+d interactions.[25]

The evidence for η' production in this final state is summarized by the scatterplot of the $(\pi^+\pi^-\pi^0/\gamma)$ mass (all four combinations are plotted) versus the $(\pi^+\pi^+\pi^-\pi^-\pi^0/\gamma)$ mass. This plot is shown in Fig. 3. The correlation of η and η' events is clear. The $(\pi^+\pi^+\pi^-\pi^-\pi^0/\gamma)$ mass plot is shown in Fig. 4; a strong η' signal occurs at a mass of 0.96 GeV/c^2 with no more than 20% background. The apparent structure near 1.1 and 1.25 GeV/c^2 coincides with the phase-space maxima for the 1.9 and 2.1 GeV/c beam momenta, respectively.

The $(\pi^+\pi^-\pi^0/\gamma)$ mass plot is shown in Fig. 5. There is a strong η signal here, much more than can be accounted for by η' decays alone. The amount of η' production was determined by estimating background and counting events in the η' and η peaks. Every event in the η' region has at least one associated $(\pi^+\pi^-\pi^0/\gamma)$ combination in the region of the η.

The amount of η' production is shown as a function of c.m. energy in Table V. The c.m. energy calculated for an event depends on the spectator momentum; since the spectator momentum for a one-constraint odd-pronged event is systematically low (see Sec. II), its c.m. energy is systematically too close to the median c.m. energy for its beam momentum. To avoid uncertainties due to the incorrectly determined c.m. energies, the c.m. energy bins were chosen to center on the median value for each beam momentum setting. Thus these events are assigned to the correct bin, even if their c.m. energy is not correctly determined.

TABLE V. Cross section for η' production.

	$E_{\text{c.m.}}$ (GeV)				
	1.94	2.02[a]	2.11[a]	2.22	2.33
Events: 3–4 prongs	11	2	24	52	21
Events: 5–6 prongs	4	17	21	19	5
Cross section (μb)	23 ± 7	91 ± 33	112 ± 30	114 ± 15	127 ± 25

[a] At 2.02 and 2.11 GeV the 3- and 4-pronged sample is incomplete. At these energies the cross section is based on 5- and 6-pronged events alone.

The amount of η' at threshold requires special discussion. When the c.m. energy is just above η' threshold (1.94 GeV) the five-pion phase space peaks at a mass of 960 MeV/c^2, with a width of 90 MeV/c^2. Also, when the five-pion mass is 960 MeV/c^2, the three-pion phase space peaks at the η mass, 550 MeV/c^2, with a width of 140 MeV/c^2. Thus background and resonance can be separated only by the narrow width of the resonance peaks. There are only 11 events in this region, so that background and resonance estimates are difficult. The lower and upper bounds for the amount of η' production (by eye) are 0 and 75%. We have also performed a maximum likelihood calculation, using a Gaussian resolution function with $\sigma = 12$ MeV/c^2 for the resonance shape, and phase-space background, which gives the amount of η' production as 36 ± 16%.

C. η' Production in Three- and Four-Pronged Events

There are three known decay modes of the η' that lead to three- and four-pronged topologies in our experiment (Reactions 12, 14, 15). We discuss here only $\eta' \to \pi^+\pi^-\eta$, $\eta \to$ neutrals, as this is the largest decay mode, and the most bias-free.

Most of the three- and four-pronged events have been analyzed elsewhere.[1,26] (The three-pronged events were not measured at all beam momenta.) The events of interest are those with a missing mass equal to the η mass (within errors), and which have no satisfactory fits to other hypotheses. We have examined this sample of events for evidence of η' production. The same cuts were made on the fiducial volume as for the five- and six-pronged events. The three- and four-pronged events were measured on the Spiral Reader, and the bubble density information was used to separate the track-mass hypotheses. The kinematic

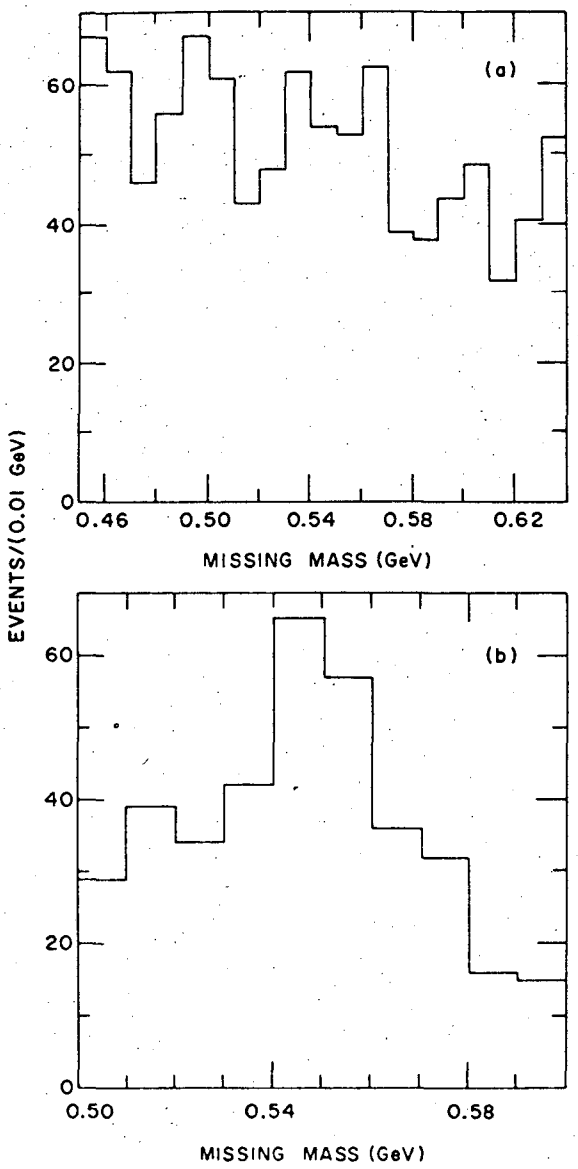

FIG. 6. Missing mass for (a) three-pronged events (978 events), (b) four-pronged events (365 events).

and ionization confidence levels for the accepted hypothesis are required to be greater than 1%. For this study, we also require that the spectator proton momentum be less than 250 MeV/c.

To separate the decay (12) from the other two modes in this topology (14, 15), we have to rely on the missing-mass measurement. The missing mass of three-pronged events with a missing mass between 0.45 and 0.64 GeV/c^2 is shown in Fig. 6(a); the missing-mass measurement. The missing a missing mass between 0.5 and 0.6 GeV/c^2 is shown in Fig. 6(b). There is no evidence for η mesons in Fig. 6(a); however, we estimate that there are 70 to 100 events in the peak at the mass of the η meson in Fig. 6(b). The resolution in

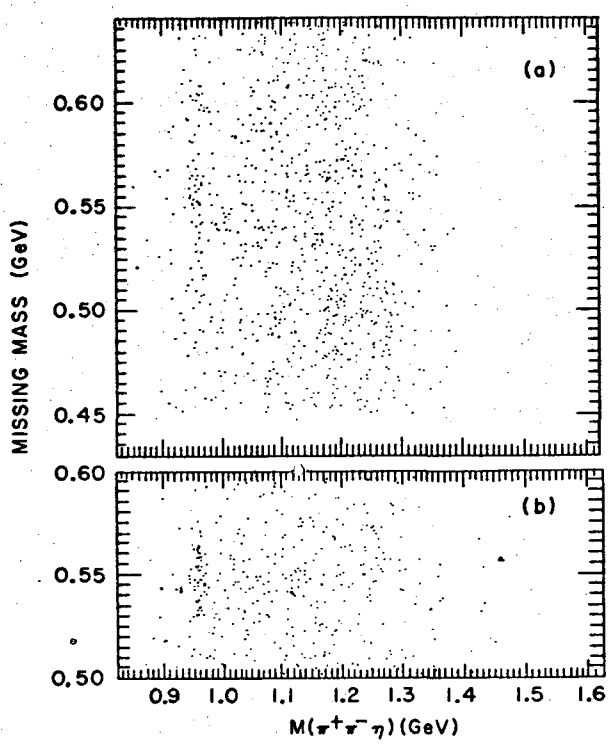

FIG. 7. Missing mass vs $M(\pi^+\pi^-\eta)$ for (a) three-pronged events (888 events), (b) four-pronged events (359 events).

missing mass in the region of the η is ± 50 MeV/c^2 for three-pronged, and ± 15 MeV/c^2 for four-pronged events.

This resolution is clearly adequate to separate γ from η, and therefore decay (15) is not expected to contaminate our sample. However, for decay (14) the missing-mass spectrum peaks near the η mass,[16] and a considerable amount of contamination from this source is expected, especially in the three-pronged sample. This contamination will not affect the η' production angular distributions to be discussed below. In order to find production cross sections, this contamination has to be taken into account.

The events shown in Fig. 6 have been fitted to the one-constraint hypothesis $\pi^+ d \to pp\pi^+\pi^-\eta$, $\eta \to$ neutrals. The scatter plot of missing mass versus $(\pi^+\pi^-\eta)$ mass is shown in Fig. 7 for the three- and four-pronged events. There is a good η' signal in both these plots; the plots also show that the background can be reduced if we make a more restrictive cut on the acceptable missing-mass range. For the rest of the analysis we require that the missing mass lie between 0.50 and 0.64 GeV/c^2 in the three-pronged events, and between 0.52 and 0.58 GeV/c^2 in the four-pronged events. With these mass cuts we estimate that about 70% of the events from decay (14) are included with the three-

pronged events, amounting to a 14% contamination of the sample. Among the four-pronged events the acceptance is about 40%, the contamination 8%.

The $(\pi^+\pi^-\eta)$ mass plot is shown in Fig. 8. The η' peak is sharp and clear here, even for the three-pronged events. The background under the η' peak is about 20% for both topologies. The amount of η' production was determined as a function of c.m. energy; the results are tabulated in Table V.

We can calculate the η' production cross section separately using the 3–4 prong and the 5–6 prong samples. Within statistics, the two samples are consistent. The ratio for the combined data from

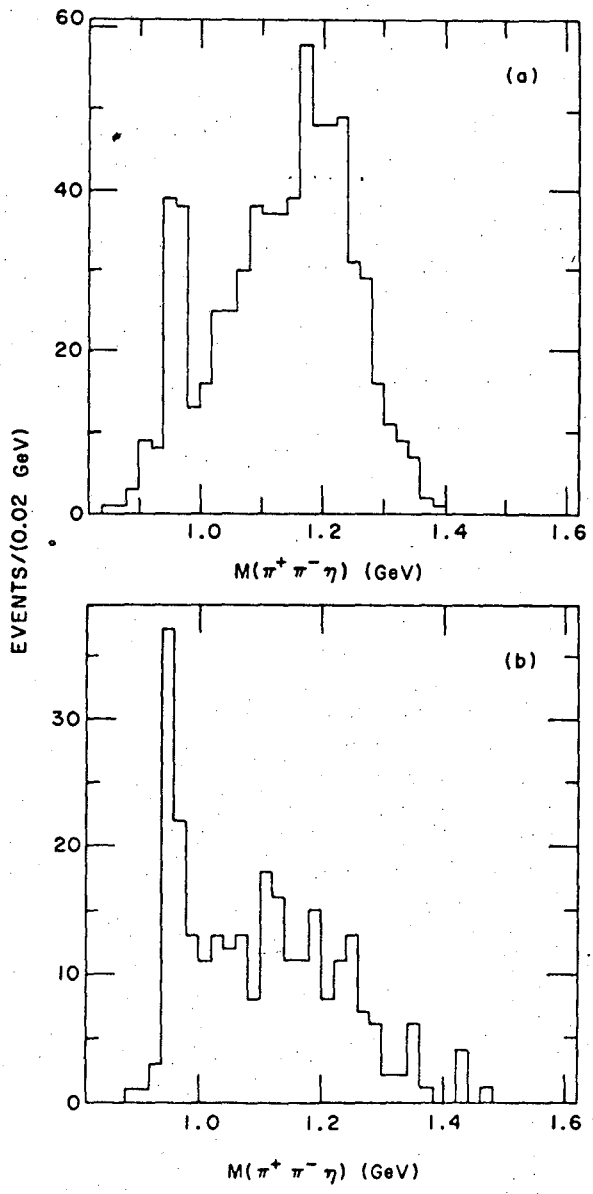

FIG. 8. Mass of $\pi^+\pi^-\eta$ for (a) fitted three-pronged events (668 events), (b) fitted four-pronged events (266 events).

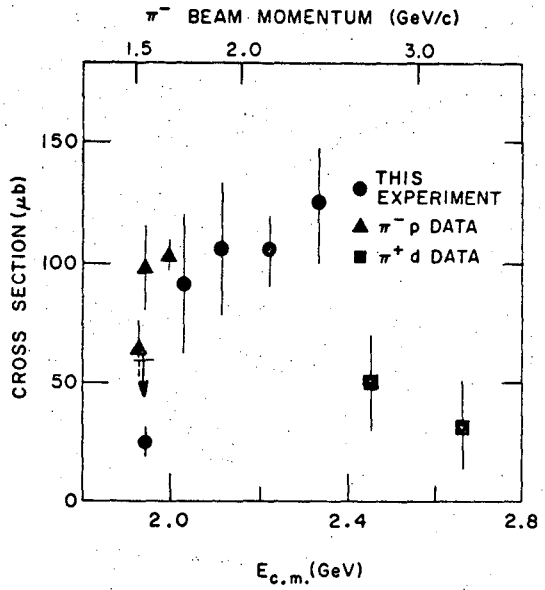

FIG. 9. Cross section for $\pi^+n \to p\eta'$; the charge-symmetric data and π^+d data from other experiments are also shown (Ref. 27).

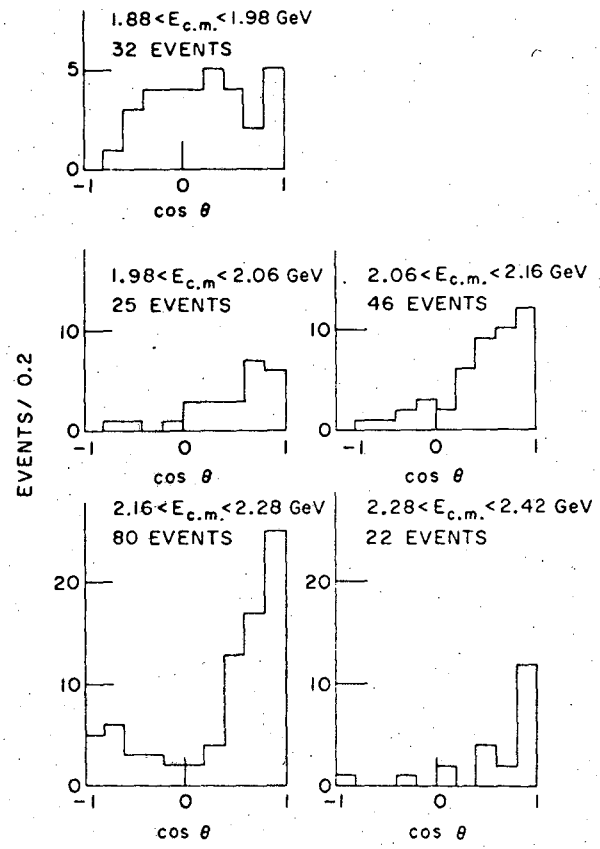

FIG. 10. Angular distribution of η' production. Data from three-, four-, five-, and six-pronged events combined.

the three energies at which we have complete samples is 1.1 ± 0.3.

D. Summary of η' Results

The cross section for η' production in $\pi^+ n$ and $\pi^- p$ interactions is shown in Fig. 9 and Table V. Our results, combined with other measurements,[27] indicate a rapid rise above threshold to a maximum of about 100 μb, and a slower decrease at higher energy.

The η' production angular distribution was studied by making a cut on the $(\pi^+\pi^-\eta)$ mass between 0.94 and 0.98 GeV/c^2. The production angular distributions for the three- and four-pronged events are consistent with each other, and with the five- and six-pronged angular distributions. The production angular distributions for the combined sample in the η' mass region are shown in Fig. 10. No corrections have been made for the effect of the background (<20%).

While the angular distribution is reasonably flat near threshold, it rapidly develops a peripheral peaking with increasing energy.

Since the cross section reaches its maximum near $E_{c.m.} = 2190$ MeV, and the width of its peak is about 300 MeV, the question arises whether or not the reaction is dominated by the process $\pi^+ n \to N^*(2190) \to \eta' p$. The amount of data available is not adequate to perform a phase-shift analysis, and therefore we cannot determine the size of the $N^*(2190)$ contribution. We note, however, that the backward peaking in the 2160–2280 MeV region is an indication that this contribution may be substantial.

The size and the energy dependence of the total cross section in the reaction we explored are similar to those found in the reaction $K^- p \to \eta' \Lambda$.[16] We suggest therefore that for future high statistics experiments designed to explore the characteristics of η' decay the reaction $\pi^- p \to \eta' n$ is an attractive one in view of the availability of high flux π^- beams in the 2-GeV/c region.

ACKNOWLEDGMENTS

This work would not have been possible without the cooperation of many people. We are especially indebted to the crews of the Bevatron and the 72-in. bubble chamber, and to our many competent scanners and measurers. The scanning and measuring were done under the supervision of Wally Hendricks.

We are grateful to Professor Luis W. Alvarez and Dr. Frank T. Solmitz for encouragement and support.

---

*This work was done under the auspices of the U. S. Atomic Energy Commission. Part of this paper is from a thesis submitted by Robert K. Rader to the Graduate Division of the University of California, Berkeley, California in partial fulfillment of the requirements for the degree of Doctor of Philosophy.

†Now at Centre d'Études Nucléaires de Saclay, Saclay, France.

‡Now at Michigan State University, East Lansing, Michigan 48823.

§Now at Brookhaven National Laboratory, Upton, New York 11973.

‖Now at Andros, Inc., Berkeley, California 94710.

**A. P. Sloan Foundation Fellow; now at State University of New York, Stony Brook, New York 11790.

††Now at Northwestern University, Evanston, Illinois 60201.

[1]Jerome S. Danburg *et al.*, Phys. Rev. D 2, 2564 (1970).

[2]Donald W. Davies *et al.*, Phys. Rev. D 2, 506 (1970).

[3]Barbara Barrett and Tran N. Truong, Phys. Rev. 147, 1161 (1966).

[4]For further details see Robert K. Rader, Lawrence Radiation Laboratory Report No. UCRL-19431, 1969 (unpublished).

[5]Gerald R. Lynch, Lawrence Radiation Laboratory Report No. UCRL-17328, 1967 (unpublished).

[6]F. T. Solmitz, A. D. Johnson, and T. B. Day, Lawrence Radiation Laboratory Physics Group A Programming Note No. P-117 (unpublished).

[7]O. I. Dahl, T. B. Day, F. T. Solmitz, and N. L. Gould, "SQUAW–Kinematic Fitting Program," Lawrence Radiation Laboratory Physics Group A Programming Note No. P-126 (unpublished).

[8]For corresponding results on three- and four-pronged events, see Ref. 1.

[9]R. L. Gluckstern and H. A. Bethe, Phys. Rev. 81, 761 (1951).

[10]M. Moravcsik, Nucl. Phys. 7, 113 (1958).

[11]The high-momentum components of the deuteron wave function are not well known, as this requires a knowledge of the amount of D-wave admixture to the predominantly S-wave wave function at small separations. Concerning the amount of D wave, see, e.g., J. S. Levinger, Phys. Letters 29B, 216 (1969), and references therein.

[12]R. G. Newton, *Scattering Theory of Waves and Particles* (McGraw-Hill, New York, 1966), Chap. 8.

[13]The cross sections for $\pi^- p \to n\pi^+\pi^+\pi^-\pi^-$ shown in Fig. 2 are given here, together with their sources:

(a) $\sigma = 0.12 \pm 0.02$ mb at 1.59 GeV/c, from Saclay-Orsay-Bari-Bologna Collaboration, Nuovo Cimento 29, 515 (1963);

(b) $\sigma = 0.34 \pm 0.11$ mb at 1.89 GeV/c, from R. Christian, A. R. Erwin, H. R. Fechter, F. E. Schwamb, S. H. Vegors, and W. D. Walker, Phys. Rev. 143, 1105 (1966);

(c) $\sigma = 0.35 \pm 0.04$ mb at 2.03 GeV/c, from D. D. Carmony, F. Grard, R. T. Van de Walle, and Nguyen-huu Xuong, in *Proceedings of the 1962 International Conference on High-Energy Physics at CERN*, edited by J. Prentki (CERN, Geneva, 1962), p. 44;

(d) $\sigma = 0.37 \pm 0.02$ mb at 2.10 GeV/c, from P. H. Satterblom, W. D. Walker, and A. R. Erwin, Phys. Rev. 134, B207 (1964);

(e) $\sigma = 0.67 \pm 0.02$ mb at 2.70 GeV/c, from P. R. Klein, R. J. Sahni, A. Z. Kovacs, and G. W. Tautfest, *ibid.* 150, 1123 (1966);

(f) $\sigma = 0.66 \pm 0.03$ mb at 2.75 GeV/c, from J. Alitti, J. P. Baton, A. Berthelot, B. Deler, W. J. Fickinger, N. Neveu-Rene, V. Alles-Borelli, R. Gessaroli, A. Romano, P. Waloschek, Nuovo Cimento 35, 1 (1965);

(g) $\sigma = 0.89 \pm 0.04$ mb at 3.2 GeV/c, from S. U. Chung, O. I. Dahl, J. Kirz, and D. H. Miller, Phys. Rev. 165, 1491 (1968);

(h) $\sigma = 1.0 \pm 0.1$ mb at 3.7 GeV/c, from Y. Y. Lee, W. D. C. Moebs, B. P. Roe, D. Sinclair, and J. C. Van der Velde, *ibid.* 159, 1156 (1967).

[14]G. R. Kalbfleisch, L. W. Alvarez, A. Barbaro-Galtieri, O. I. Dahl, P. Eberhard, W. E. Humphrey, J. S. Lindsay, D. W. Merrill, J. J. Murray, A. Rittenberg, R. R. Ross, J. B. Shafer, F. T. Shively, D. M. Siegel, G. A. Smith, and R. D. Tripp, Phys. Rev. Letters 12, 527 (1964).

[15]M. Goldberg, M. Gundzik, J. Leitner, M. Primer, P. L. Connolly, E. L. Hart, K. W. Lai, G. W. London, N. P. Samios, and S. S. Yamamoto, Phys. Rev. Letters 13, 249 (1964).

[16]Alan Rittenberg, Lawrence Radiation Laboratory Report No. UCRL-18863, 1969 (unpublished); J. P. Dufey, B. Gobbi, M. A. Pouchon, A. M. Cnops, G. Finocchiaro, J. C. Lassalle, P. Mittner, and A. Müller, Phys. Letters 29B, 605 (1969).

[17]Particle Data Group, Rev. Mod. Phys. 43, S1 (1971).

[18]G. H. Trilling, J. L. Brown, G. Goldhaber, S. Goldhaber, J. A. Kadyk, and J. Scanio, Phys. Letters 19, 427 (1965).

[19]J. P. Dufey, B. Gobbi, M. A. Pouchon, A. M. Cnops, G. Finocchiaro, J. C. Lassalle, P. Mittner, and A. Müller, Phys. Letters 26B, 410 (1968).

[20]E. Hyman, W. Lee, J. Peoples, J. Schiff, C. Schultz, and S. Stein, Phys. Rev. 165, 1437 (1968).

[21]M. Basile, D. Bollini, P. Dalpiaz, P. L. Frabetti, T. Massam, F. Navach, F. L. Navarria, M. A. Schneegans, and A. Zichichi, Nuovo Cimento 3A, 371 (1971).

[22]H. O. Cohn, R. D. McCulloch, W. M. Bugg, and G. T. Condo, Phys. Letters 21, 347 (1966).

[23]T. C. Bacon, W. J. Fickinger, D. G. Hill, H. W. K. Hopkins, D. K. Robinson, and E. O. Salant, Phys. Rev. 157, 1263 (1967).

[24]R. J. Miller, S. Lichtman, and R. B. Willmann, Phys. Rev. 178, 2061 (1969).

[25]M. Aguilar-Benitez, D. Bassano, R. L. Eisner, J. B. Kinson, D. Pandoulas, N. P. Samios, and V. E. Barnes [Phys. Rev. Letters 25, 1635 (1970)] indicate that there may exist another boson, M, near the η' (with a mass 953 ± 2 MeV) which also decays into $\pi\pi\eta$ and $\pi\pi\gamma$. If the M is confirmed, and is produced in $\pi^+ n$ interactions, our results refer to the sum of the η' and the M.

[26]Robert J. Manning, Lawrence Radiation Laboratory Report No. UCRL-19339, 1969 (unpublished).

[27]The cross sections for $\pi^- p \to n\eta'$, and $\pi^+ d \to pp\eta'$ shown in Fig. 9 are as follows:

(a) $\sigma < 60$ μb, $\pi^- p$ at 1.5 GeV/c, from Ref. 20;

(b) $\sigma = 65 \pm 12$ μb, $\pi^- p$ at 1.50 GeV/c, and $\sigma = 98 \pm 18$ μb, $\pi^- p$ at 1.52 GeV/c, from Ref. 19;

(c) $\sigma = 50 \pm 20$ μb, $\pi^+ d$ at 2.7 GeV/c, from Ref. 24;

(d) $\sigma = 30^{+18}_{-22}$ μb, $\pi^+ d$ at 3.29 GeV/c, from Ref. 22;

(e) $\sigma = 108 \pm 14$ μb, $\pi^- p$ at 1.61 GeV/c from Ref. 21.

TECHNICAL INFORMATION DIVISION
LAWRENCE BERKELEY LABORATORY
UNIVERSITY OF CALIFORNIA
BERKELEY, CALIFORNIA 94720